PNAS
www.pnas.org

Supplementary Information for

Predominant localization of phosphatidylserine at the cytoplasmic leaflet of the ER, and its TMEM16K-dependent redistribution

Takuma Tsuji, Jinglei Cheng, Tsuyako Tatematsu, Aoi Ebata, Hiroki Kamikawa, Akikazu Fujita, Sayuri Gyobu, Katsumori Segawa, Hiroyuki Arai, Tomohiko Taguchi, Shigekazu Nagata, and Toyoshi Fujimoto

Toyoshi Fujimoto
Email: tfujimot@med.nagoya-u.ac.jp

This PDF file includes:

www.pnas.org/cgi/doi/10.1073/pnas.1822025116

Supplementary materials and methods

Probes

Two copies of the PH domain of human evectin-2 were cloned into a pGEX-6P vector (GE Healthcare) in tandem. Recombinant proteins were produced in *E. coli* BL21 (DE3), affinity-purified using glutathione-agarose (Sigma), and eluted with a glutathione solution.

A hamster anti-mouse TMEM16K antibody (Ab) was generated as described (1). Rabbit anti-GST (Bethyl), mouse anti-GST (BioLegend), rabbit anti-cytochrome P450 reductase (POR) (Stressgen), rabbit anti-Rab11 (Thermo Fisher), rabbit anti-lamin B1 (Abcam), and mouse anti-Flag (Sigma) Abs were purchased. Colloidal gold particles conjugated with protein A (The University Medical Center Utrecht), goat anti-rabbit IgG Ab (BB International), and goat anti-mouse IgG Ab (Jackson ImmunoResearch), were also purchased.

Liposomes

Phosphatidylcholine (1-palmitoyl-2-oleoyl-sn-glycero-3-phosphocholine) (Nichiyu), L-α-phosphatidylserine (bovine brain), L-α-phosphatidylethanolamine (bovine liver) (Olbracht Serdary), and L-α-phosphatidylinositol (bovine liver) (Avanti) were dissolved in chloroform/methanol (2:1) at defined molar ratios, dried by dry nitrogen gas, and vortexed with an aqueous buffer to generate liposomes. The liposome solution was pushed through a Mini-extruder (Avanti) equipped with a polycarbonate membrane filter (pore size, 0.2 μm) to generate unilamellar vesicles.

Proteinase K treatment

Some replicas were treated overnight at 37ºC with 50 μg/ml proteinase K (TAKARA) in 20 mM Tris-HCl (pH8.0), 10 mM EDTA, 10 mM NaCl, and 0.5% SDS. The replicas were rinsed extensively with 2.5% SDS in 0.1 M Tris-HCl (pH 8.0) and then PBS containing 0.1% Tween-20 before being subjected to labeling.

Quantitative real-time PCR

Total RNA was extracted from MEFs and from mouse quadriceps muscle using the ReliaPrep RNA Cell Miniprep System (Promega). cDNA was obtained using Superscript

III reverse transcriptase (Thermo Fisher). qRT-PCR was performed using the Brilliant III Ultra-Fast SYBR Green QPCR Master Mix with Low ROX (Agilent Technologies) and an Mx3005P real-time PCR system (Agilent Technologies) according to the manufacturer's instructions. The primer sequences for TMEM16E, TMEM16K, and β-actin were described before (2).

cDNA transfection

Retrovirus vectors were prepared in PLAT-E cells using the pMXs-IRES-puro vector, both of which were provided by Dr. Toshio Kitamura (3). MEFs stably expressing the protein were selected by resistance to puromycin. The vectors for GFP-cytochrome b5 (4) and calnexin-N-14-mApple were obtained from Addgene.

Fluorescence microscopy

For immunofluorescence microscopy, cells fixed with 3% formaldehyde were permeabilized with 0.5% Triton X-100 and labeled with an anti-FLAG antibody. Images were captured by an Axio Imager 2 equipped with Apotome2 (Carl Zeiss) using a Plan-Neofluar 100x/1.30. For Ca^{2+} imaging, cells cultured in a glass-bottom dish were loaded with 3 μM of Fluo-4-AM (Dojindo) in DMEM supplemented with 10% FCS for 20 min, and washed with DMEM supplemented with 10% FCS and then with HBSS containing 2.5 mM $CaCl_2$. Cells were treated with or without A23187 at 37ºC, and observed by an Axio Observer (Carl Zeiss) using a Plan-Neofluar 63x/1.35. ΔF was calculated as described before (5).

Box plots

Box plots were prepared using BoxPlotR (http://boxplot.tyerslab.com/). The center lines show the median, box boundaries indicate the 25th and 75th percentiles, whiskers delineate maximum and minimum data points that are no more than 1.5 times the interquartile range, and dots represent individual data points.

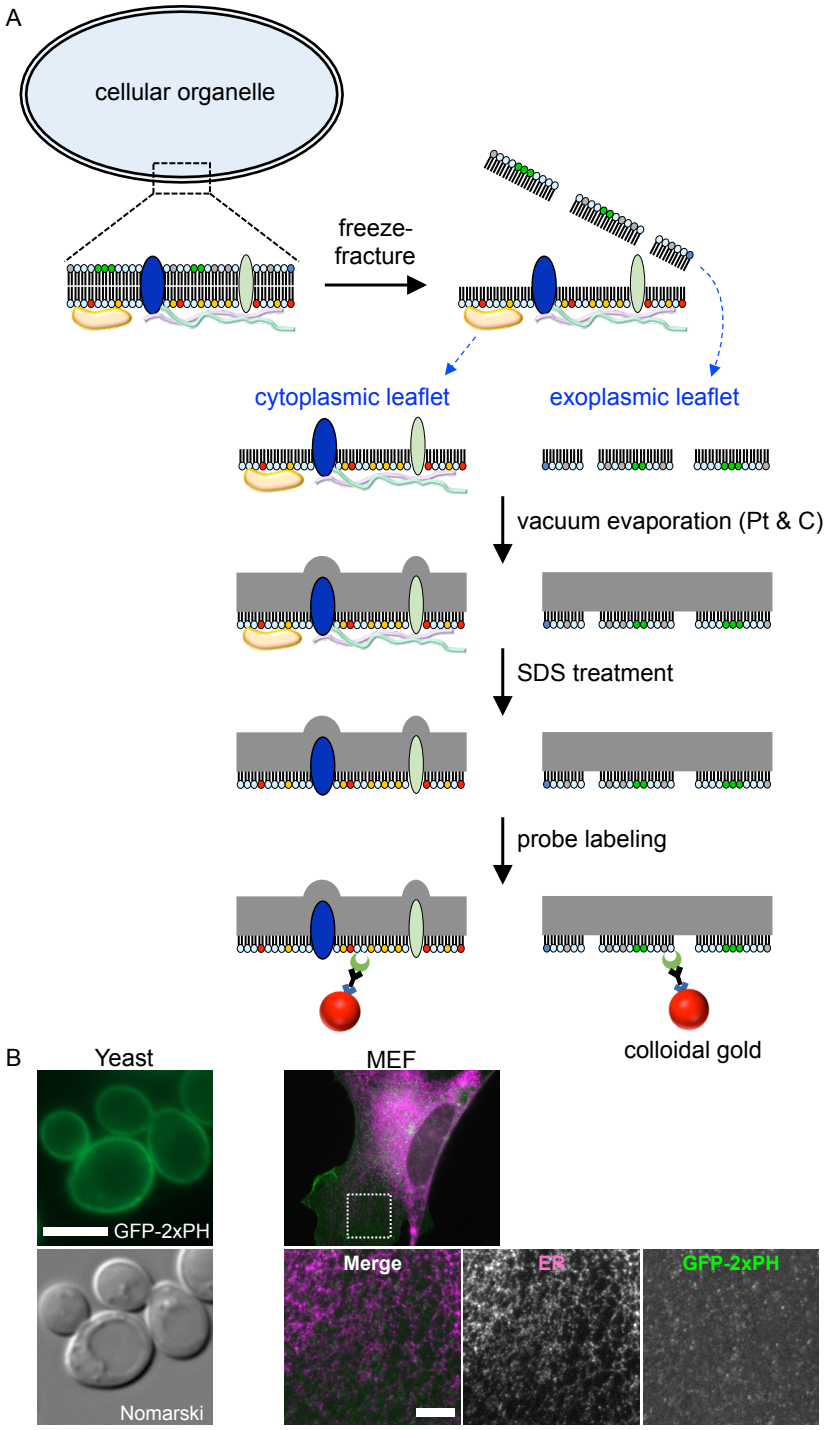

Fig. S1. Methodology. (*A*) Summary of the QF-FRL method. Live cells are quickly frozen by high-pressure freezing, and subjected to freeze-fracture, which splits the membranes into two leaflets. Vacuum evaporation of platinum and carbon at an ultra-low temperature (below –100ºC) physically stabilizes the lipids in the split leaflets. The specimen, called the "freeze-fracture replica," is treated with an SDS solution to dissolve peripheral membrane proteins, and incubated with GST-2xPH, followed by an anti-GST antibody and colloidal gold-conjugated protein A. The colloidal gold particles (5 to 10 nm in diameter) are observed under EM. (*B*) Distribution of GFP-tagged 2xPH expressed in yeast and MEF. The ER in MEF was visualized by expression of calnexin-N-14-mApple. Bars, 5 μm.

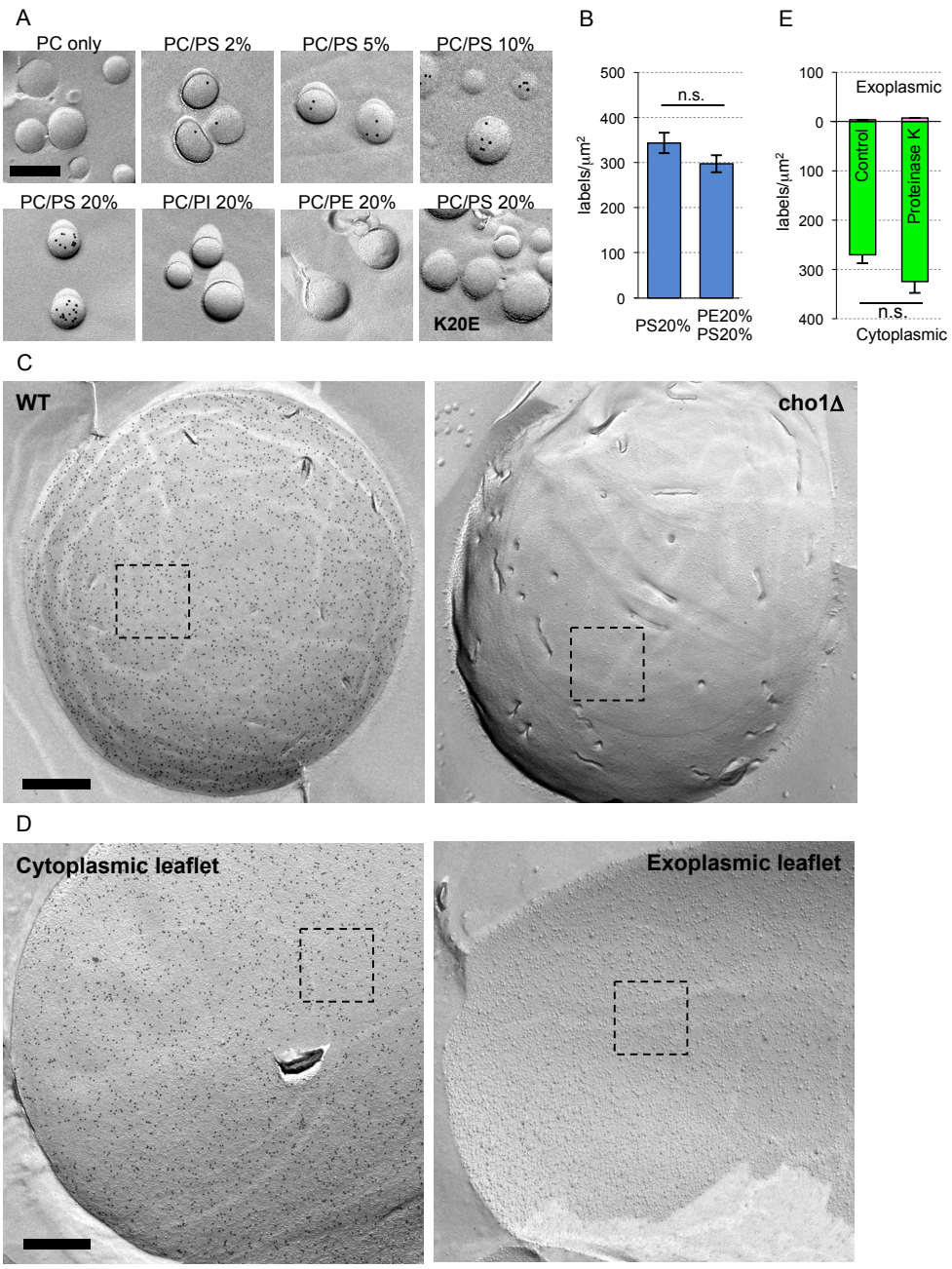

Fig. S2. Validation of the QF-FRL procedure. (*A*) Freeze-fracture replicas were prepared with liposomes composed of phosphatidylcholine (PC) only, or of PC with the indicated concentration of PtdSer (PS), phosphatidylethanolamine (PE), or phosphatidylinositol (PI), and labeled with GST-2xPH or GST-2xPH(K20E). Bar, 0.2 μm. (*B*) Liposomes containing 20% PS were prepared with or without 20% PE and compared in the labeling intensity with GST-2xPH. Gold particles/μm^2. Mean ± SEM (n > 100). n.s., not significant. (*C*) Labeling of PtdSer in the cytoplasmic leaflet of the plasma membrane in wild-type (WT) and *cho1Δ* yeast. Bar, 0.5 μm. The areas enclosed by the dotted squares are shown in Fig. 1*B*. (*D*) PtdSer labeling of the cytoplasmic and exoplasmic leaflets of human red blood cells. Bar, 0.5 μm. The areas enclosed by dotted squares are shown in Fig. 1*C*. (*E*) Freeze-fracture replicas of human red blood cell membrane, treated with or without proteinase K, were labeled with GST-2xPH and compared in labeling intensity (gold particles/μm^2). Bar, 0.5 μm. Mean ± SEM (n = 10).

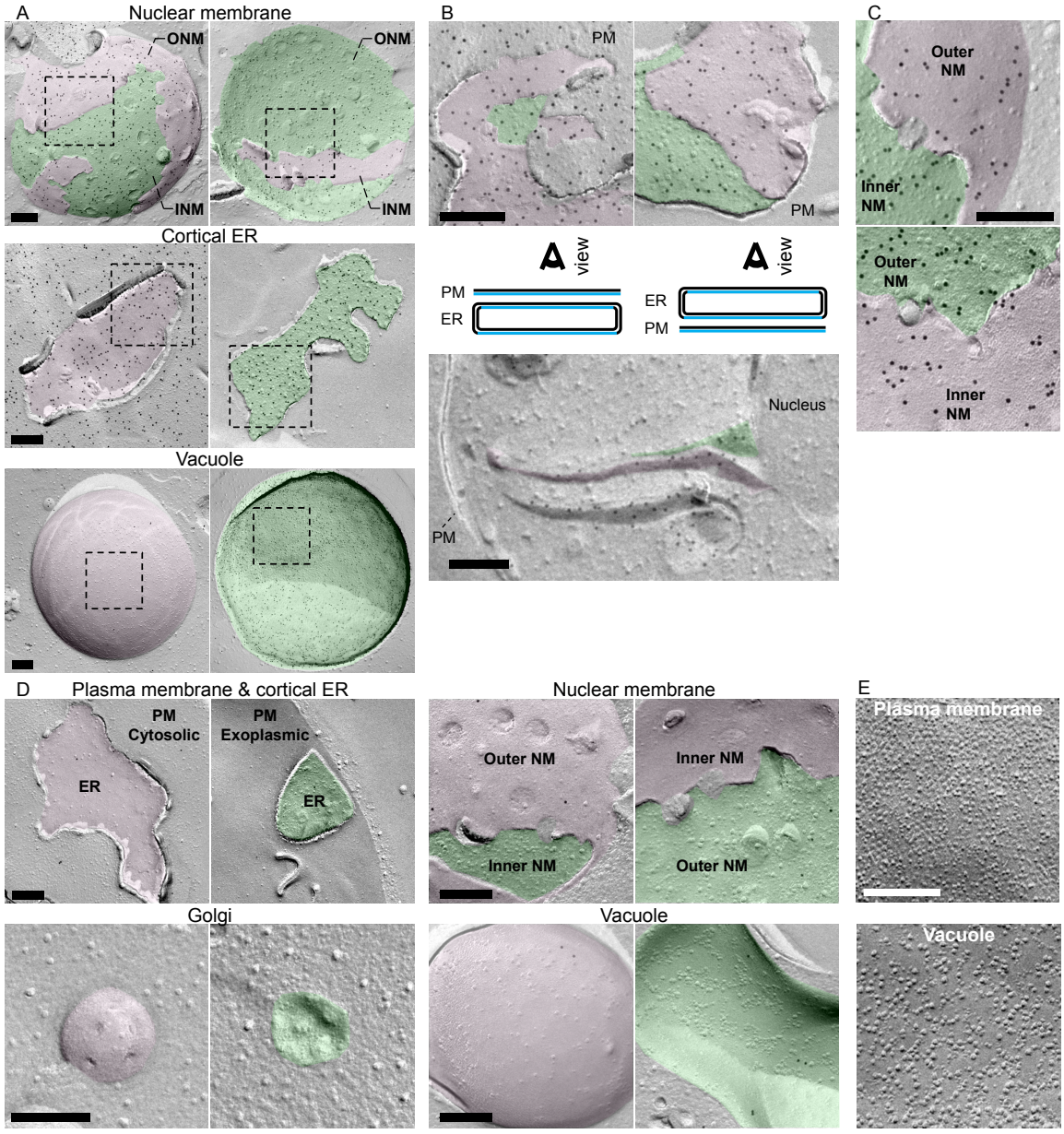

Fig. S3. Localization of PtdSer in yeast. The intracellular PtdSer distribution in yeast was examined by QF-FRL. The cytoplasmic leaflet and the exoplasmic leaflet are colored in green and pink, respectively. (*A*) Localization of PtdSer in the NMs, cortical ER, and vacuole in wild-type yeast. Bars, 0.2 μm. The areas enclosed by dotted squares are shown at a higher magnification in Fig. 2*A*. (*B*) Localization of PtdSer in the cortical ER (upper figures) and the cytoplasmic ER extending from the NM (lower figure). The middle drawings show the view angle for the upper left and right figures. Bars, 0.2 μm. (*C*) Labeling in the nuclear membrane after proteinase K treatment. Bar, 0.2 μm. (*D*) Little PtdSer labeling in the plasma membrane, cortical ER, NMs, Golgi, and vacuole in *cho1Δ* yeast. Bars, 0.2 μm. (*E*) Freeze-fracture EM of the plasma membrane and the vacuole. The density of intramembrane particles, which largely represent transmembrane proteins, was much higher in the plasma membrane than in the vacuole. Bar, 0.1 μm.

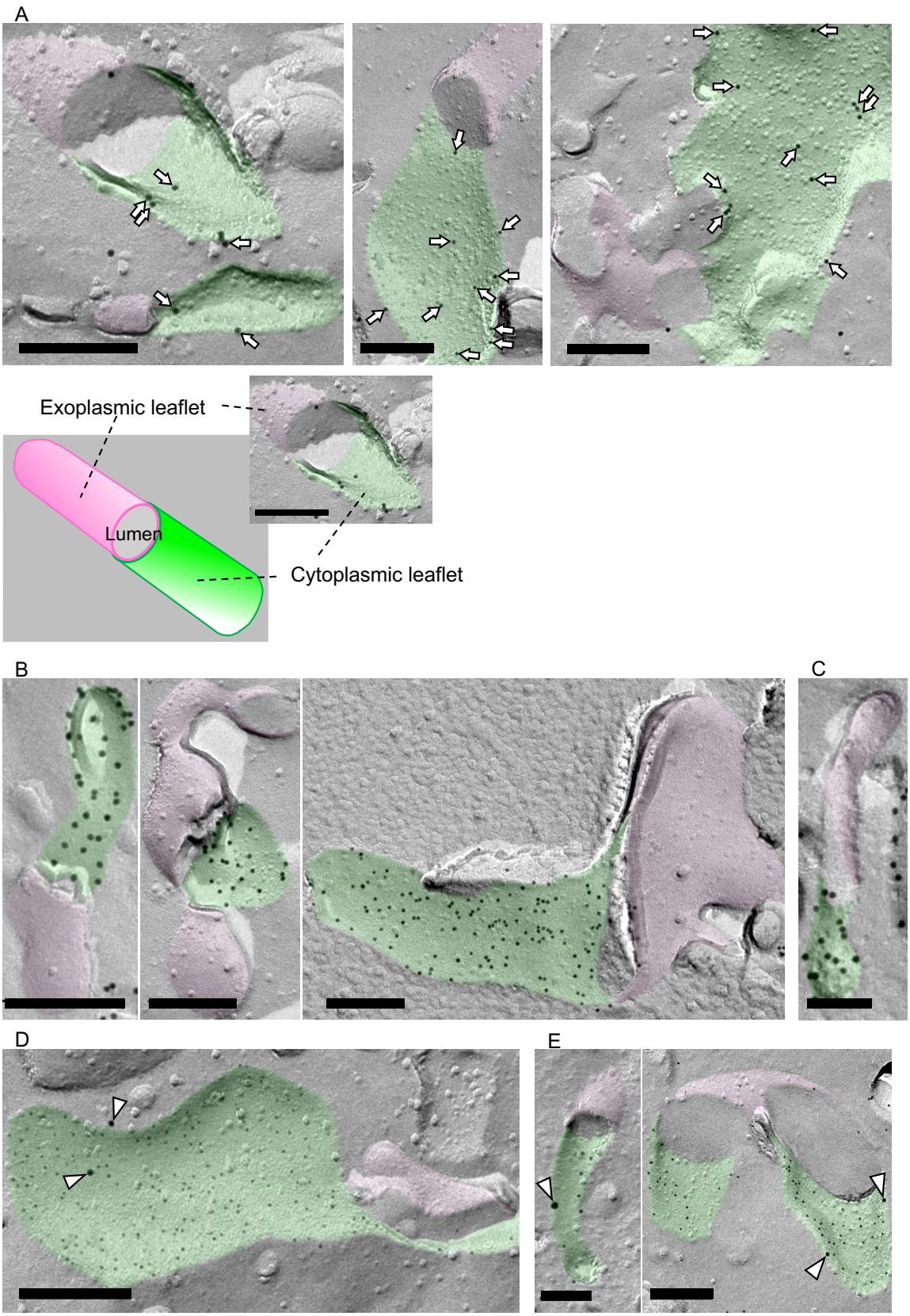
A
Exoplasmic leaflet
Lumen
Cytoplasmic leaflet
B
C
D
E

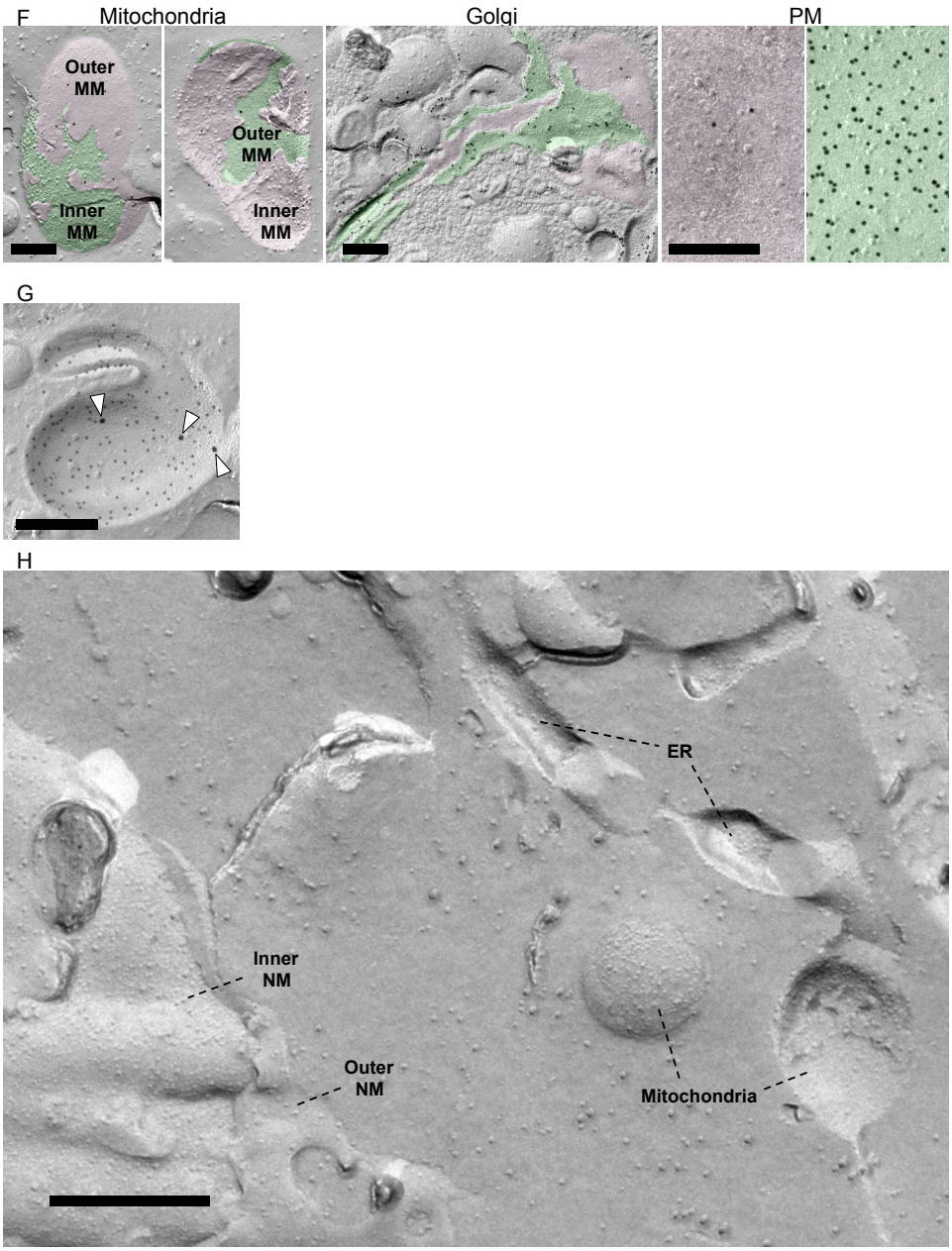

Fig. S4. Localization of PtdSer in mammalian cells. The intracellular PtdSer distribution in mouse and rat cells was determined by QF-FRL. The cytoplasmic and exoplasmic leaflets are colored in green and pink, respectively. (*A*) Immunolabeling of MEFs with an antibody against P450 reductase (POR) (arrows), which is localized to the ER. Membranes with a tubular or sheet-like structure with a narrow lumen are ER. Bars, 0.2 μm. The diagram shows that the cytoplasmic and exoplasmic leaflets can be determined unambiguously when the ER is observed as three-dimensional tubules or cisterns. (*B*) Labeling of PtdSer in MEFs on an ER membrane with tubular and sheet-like structures. Bars, 0.2 μm. (*C*) Labeling in the ER after proteinase K treatment. Bar, 0.1 μm. (*D*) Double labeling for PtdSer and POR in MEFs. Small (6 nm) and large (12 nm; arrowheads) colloidal gold particles labeled PtdSer and POR, respectively. Bar, 0.2 μm. (*E*) Double labeling for PtdSer (6 nm) and POR (12 nm; arrowheads) in rat McA-RH7777 cells. Bar, 0.1 μm (left panel); 0.2 μm (right panel). (*F*) PtdSer labeling in MEFs in the mitochondria, Golgi, and plasma membrane (PM). Bars, 0.2 μm. (*G*) Double labeling in MEFs for PtdSer (6 nm) and Rab11 (12 nm; arrowheads). Bar, 0.2 μm. (*H*) Labeling with GST-2xPH(K20E) in an MEF. Bar, 0.5 μm.

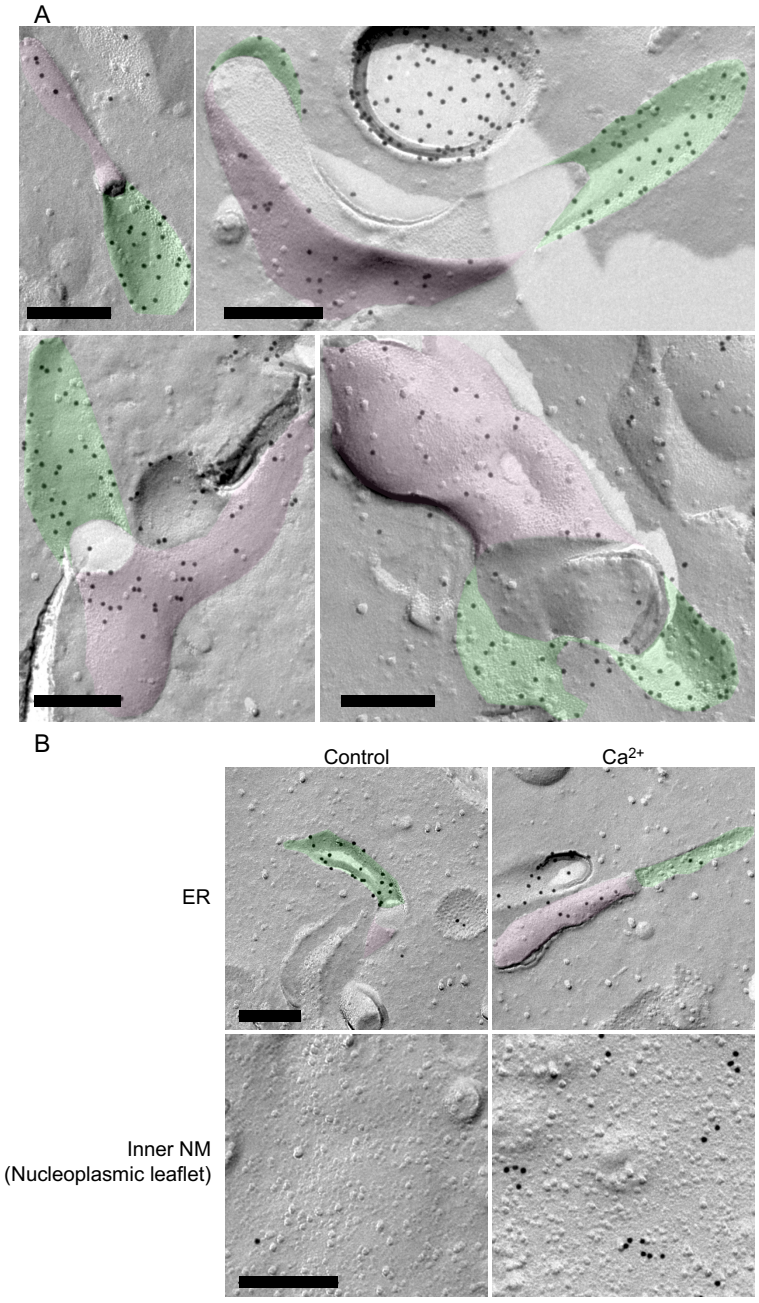

Fig. S5. Re-distribution of PtdSer upon treatment with A23187. (*A*) PtdSer labeling in the ER of MEFs after A23187 treatment. Bars, 0.2 μm. (*B*) PtdSer labeling in McA-RH7777 cells under normal culture condition (control) and after A23187 treatment (Ca^{2+}). Bars, 0.2 μm. The cytoplasmic and exoplasmic leaflets are colored in green and pink, respectively.

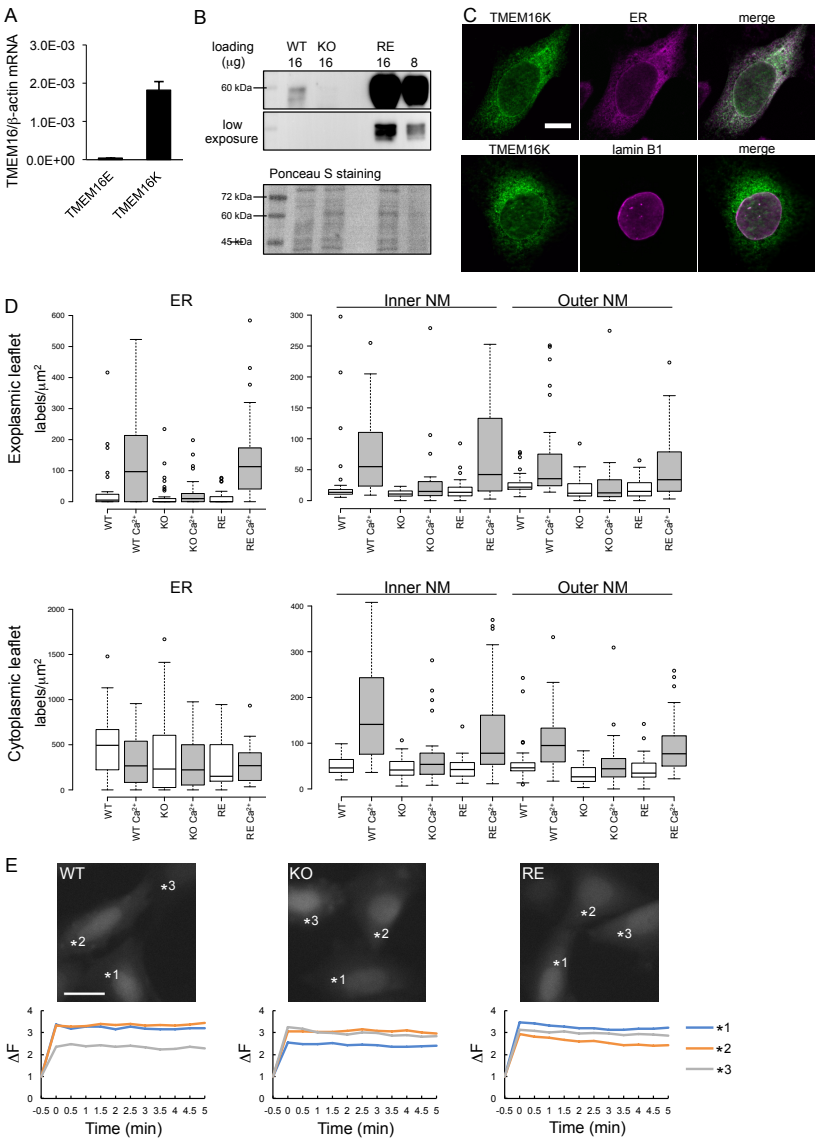

Fig. S6. Effect of TMEM16K on the Ca^{2+}-induced redistribution of PtdSer in MEF. (*A*) Quantitative RT-PCR for TMEM16E and 16K mRNAs. The mRNA levels of TMEM16E and TMEM16K in MEFs were determined by Real Time RT-PCR, and are expressed relative to β-actin mRNA. (*B*) Western blotting with an anti-TMEM16K antibody. Wild-type (WT), *TMEM16K*$^{-/-}$ (KO), and *TMEM16K*$^{-/-}$ MEF transformants expressing TMEM16K (RE). (*C*) Localization of TMEM16K in the ER and NMs. MEF transformants expressing Flag-tagged TMEM16K were stained with an anti-Flag antibody (Green). The ER and the NMs (magenta) were marked by expressing mCherry-cytochrome b5 and by staining with an anti-lamin B1 Ab, respectively. Merged images of the Flag and mCherry signals, and of the Flag and lamin B1 signals, are shown at right. Bar, 10 μm. (*D*) PtdSer-labeling density in the wild-type and *TMEM16K*$^{-/-}$ MEFs with or without A23187 treatment. Wild-type (WT), *TMEM16K*$^{-/-}$ (KO), and *TMEM16K*$^{-/-}$ MEF transformants expressing TMEM16K (RE) were left untreated or treated with A23187 (Ca^{2+}), and analyzed by QF-FRL. The PtdSer-labeling density in the exoplasmic and cytoplasmic leaflets of the ER, the inner NM, and the outer NM are shown. The data were obtained from three independent experiments. n >30. Center lines show the median, box boundaries indicate the 25th and 75th percentiles, whiskers delineate maximum and minimum data points that are no more than 1.5 times the interquartile range, and dots represent individual data points. The same data are presented in Figs. 4*A*, 4*B*, and 5*A* in other formats. (*E*) Fluo-4 fluorescence intensity of wild-type (WT), *TMEM16K*$^{-/-}$ (KO), and *TMEM16K*$^{-/-}$ MEF transformants expressing TMEM16K (RE) before and after the A23187 treatment. The fluorescence intensity measured in the numbered areas in the micrographs is shown in the graph.

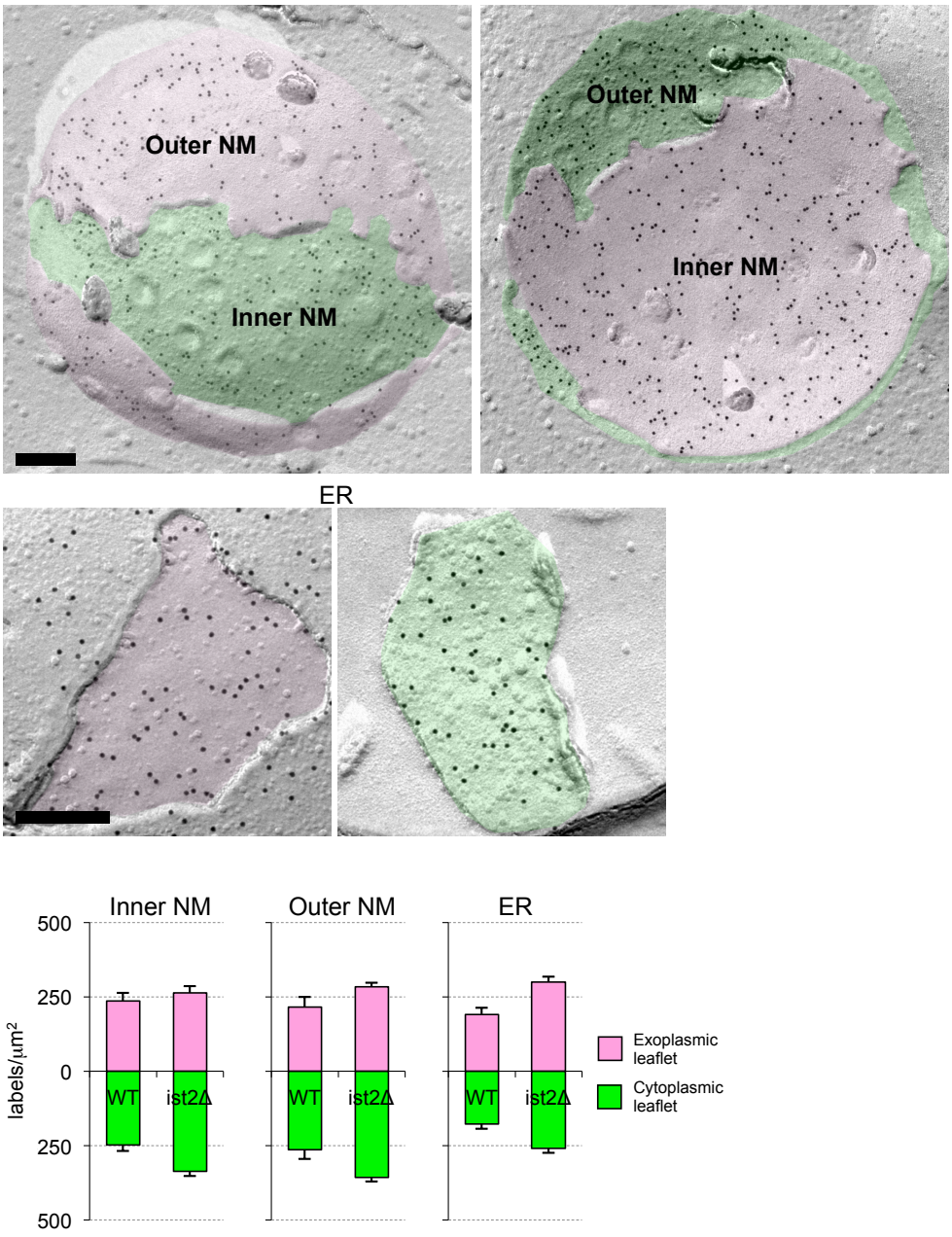

Fig. S7. No effect of the *ist2Δ* mutation on the PtdSer distribution in yeast. The yeast *ist2Δ* mutant was analyzed by QF-FRL, and the PtdSer labeling profile in the NMs and the ER are shown. Bars, 0.2 μm. In the lower panel, the PtdSer labeling density in the exoplasmic and cytoplasmic leaflets of the inner NM, the outer NM, and the ER was compared for the wild-type and *ist2Δ* yeast.

Table S1. The proportion of PtdSer in the total lipids calculated from the present results and reported biochemical results.

		Plasma membrane	Vacuole	Reference
a	PtdSer labeling density	294	322	This study
b	PtdSer/phospholipid (mol%)	33.6	4.4	(6)
c	ergosterol/protein (mg/mg)	0.40	0.05	(6)
d	ergosterol/phospholipid (mol/mol)	3.31	0.18	(6)
e	sphingolipid/protein (nmol/mg)	225.3	185.4	(7)
f	ergosterol/protein (nmol/mg)	1008	126	**c**, molecular weight of ergosterol = 396.65
g	ergosterol/sphingolipid (mol/mol)	4.47	0.68	**e, f**
h	phospholipid/ergosterol/sphingolipid	1/3.31/0.74	1/0.18/0.27	**d, g**
i	PtdSer/total membrane lipid (mol%)	6.65	3.04	**b, h**

See *SI Appendix*, Figure S3*E* for the freeze-fracture EM showing the higher density of transmembrane proteins in the plasma membrane than in the vacuole.

References

1. Ishihara K, Suzuki J, & Nagata S (2016) Role of Ca(2+) in the stability and function of TMEM16F and 16K. *Biochemistry* 55:3180-3188.
2. Suzuki J*, et al.* (2013) Calcium-dependent phospholipid scramblase activity of TMEM16 protein family members. *J Biol Chem* 288:13305-13316.
3. Onishi M*, et al.* (1996) Applications of retrovirus-mediated expression cloning. *Exp Hematol* 24:324-329.
4. Itakura E & Mizushima N (2010) Characterization of autophagosome formation site by a hierarchical analysis of mammalian Atg proteins. *Autophagy* 6:764-776.
5. Johnson RD, Schauerte JA, Wisser KC, Gafni A, & Steel DG (2011) Direct observation of single amyloid-beta(1-40) oligomers on live cells: binding and growth at physiological concentrations. *PLoS One* 6:e23970.
6. Zinser E*, et al.* (1991) Phospholipid synthesis and lipid composition of subcellular membranes in the unicellular eukaryote Saccharomyces cerevisiae. *J Bacteriol* 173:2026-2034.
7. Hechtberger P*, et al.* (1994) Characterization, quantification and subcellular localization of inositol-containing sphingolipids of the yeast, Saccharomyces cerevisiae. *Eur J Biochem* 225:641-649.